Journal of Vacuum Science and Technology A

RESEARCH ARTICLE | MARCH 21 2025

Generation of ultra-low work function surfaces by caesium and water coadsorption in view of negative hydrogen ion sources

A. Heiler ; N. Klose ; R. Friedl ; U. Fantz ; D. Vlachos

J. Vac. Sci. Technol. A 43, 033203 (2025)
https://doi.org/10.1116/6.0004354

JVST A
Journal of Vacuum Science & Technology A

ARTICLE

pubs.aip.org/avs/jva

Generation of ultra-low work function surfaces by caesium and water coadsorption in view of negative hydrogen ion sources

Cite as: J. Vac. Sci. Technol. A 43, 033203 (2025); doi: 10.1116/6.0004354
Submitted: 29 December 2024 · Accepted: 21 February 2025 ·
Published Online: 21 March 2025

A. Heiler,[1,a] N. Klose,[1,2] R. Friedl,[2] U. Fantz,[1,2] and D. Vlachos[3]

AFFILIATIONS

[1]Max-Planck-Institut für Plasmaphysik (IPP), Boltzmannstr. 2, Garching D-85748, Germany
[2]AG Experimentelle Plasmaphysik, Universität Augsburg, Augsburg D-86135, Germany
[3]Department of Physics, University of Ioannina, Ioannina GR-451 10, Greece

[a]**Author to whom correspondence should be addressed:** adrian.heiler@ipp.mpg.de

ABSTRACT

The surface production of negative hydrogen ions requires low work function (WF) converter surfaces, for which caesium adsorption is typically used. Since caesium is highly reactive and easily forms caesium compounds, the resulting WF is strongly influenced by the vacuum conditions, ranging from about 10^{-8} to 10^{-6} mbar in present-day negative hydrogen ion sources for accelerators and fusion. As water is usually the main residual gas, dedicated investigations on the WF evolution upon caesium and water coadsorption are performed. The investigations are conducted in an ultra-high vacuum chamber (base pressure of $\sim 10^{-10}$ mbar), where a polycrystalline molybdenum surface is caesiated and water is admitted by using a variable leak valve. Up to a water pressure of 10^{-9} mbar, the typical WF minimum curve is measured: The WF decreases to 1.5 ± 0.1 eV in the submonolayer regime and increases to 1.8 ± 0.1 eV for longer caesiation times. For water pressures $\gtrsim 10^{-8}$ mbar, the WF decreases to below 1.5 eV for a sufficient caesium flux onto the surface, indicating the formation of caesium oxides. The WF stabilizes at 1.2 ± 0.1 eV and is in agreement with measurements performed in a high vacuum chamber (base pressure of $10^{-6} - 10^{-5}$ mbar), where it is shown that the ultra-low WF is achieved for a caesium to water flux ratio of $\gtrsim 5 \times 10^{-3}$ onto the surface. Heating the substrate to temperatures above 200 °C leads to caesium desorption from the surface and to a WF increase of the ultra-low WF layer. The results impressively demonstrate that the base pressure and applied surface temperature are decisive parameters for the development of negative hydrogen ion sources.

I. INTRODUCTION

The adsorption of alkali metals on surfaces is a well-known method for reducing the surface work function (WF).[1–3] In negative hydrogen ion sources, the alkali metal caesium (Cs) is commonly used to lower the WF of the plasma facing the first electrode (converter surface) of a multielectrode extraction and acceleration system. The WF reduction is required to provide an efficient surface production of negative hydrogen ions (see Ref. 4 and references therein). Cs is chosen as it has the lowest WF of all stable elements ($2.0 - 2.1$ eV)[5,6] and can easily be introduced into the ion source via evaporation from a Cs oven.

The WF change of metal surfaces upon Cs adsorption has been studied mostly under ultra-high vacuum (UHV) conditions with base pressures of $\leq 10^{-9}$ mbar.[7–11] It is found that for low Cs coverage, the WF decreases almost linearly upon Cs adsorption. At about $0.5 - 0.7$ monolayer (ML), the decrease slows down and the WF reaches a minimum of $1.5 - 1.6$ eV. Afterward, the WF increases and the value of bulk Cs is approached. This characteristic WF minimum curve occurs due to the gradual build up of electrostatic dipoles (outward to the surface) induced by Cs chemisorption bonds, which lower the WF. With increasing Cs coverage, however, the Cs adatoms interact with each other and the WF increases due to depolarization effects.[12,13] For coverages of $\gtrsim 1$ ML, covalent interactions between the Cs adatoms begin to get dominant and a metallization of the Cs overlayer takes place.[14,15] Nevertheless, due to the high vapor pressure of Cs, the

growth of Cs multilayers at room temperature is usually not achieved.[1]

At present, negative hydrogen ion sources for accelerators and fusion based on surface production operate with a typical base pressure in the range of $10^{-8} - 10^{-6}$ mbar,[16] i.e., Cs deposition takes place under non-UHV conditions. Therefore, the amount of coadsorbates (mainly water vapor and small amounts of oxygen and nitrogen) is not negligible. Interactions of Cs with residual gases occur predominantly at the surfaces, as the mean free path of Cs ($\sim 10^2 - 10^4$ m) is much larger than the experimental dimensions. Due to the high chemical reactivity of Cs, Cs compounds are easily formed and thus lead to a different Cs chemistry and WF compared to UHV conditions. In addition, the hydrogen plasma species (in particular, VUV photons, H atoms, and positive hydrogen ions) during plasma phases (operational phase for negative hydrogen ion production and extraction) have a significant influence on the WF of caesiated surfaces, which is described in detail in Ref. 17.

As the main residual gas in ion sources is typically water, the interaction of Cs with H_2O is of high importance with regard to the chemical composition and WF of the converter surface. In general, Cs is a well-known getter material,[5] and the presence of Cs atoms on metal surfaces promotes water adsorption. Water molecules can nucleate around the Cs atoms forming complexes,[18] which are stabilized by hydrogen bondings. Furthermore, Cs atoms enhance the partial and full dissociation of water molecules at the surface, which is dependent on the substrate material, temperature, and Cs coverage.[19–21] The formation of Cs compounds is generally favored from an energetic point of view because the bond dissociation energies of Cs−OH, Cs−O, and Cs−H bonds are higher than the dissociation energy for Cs and H_2O bonds, and the standard enthalpy of formation is negative for Cs compounds with oxygen and/or hydrogen.[5] In the case of partial dissociation, the formation of Cs hydroxide (CsOH) is likely, and when atomic oxygen is present due to the full dissociation of H_2O, a whole series of Cs oxides can be formed: Apart from Cs monoxide (Cs_2O), various suboxides (e.g., $Cs_{11}O_3$, Cs_7O, and Cs_4O), and oxygen-rich compounds such as Cs peroxide (containing O_2^{2-}), Cs superoxide (containing O_2^-), and Cs ozonide (containing O_3^-) exist.[22] By the controlled coadsorption of Cs and oxygen under UHV conditions, it was found that the formation of Cs oxides allows the generation of ultra-low WFs of below 1.5 eV. In the case of Cs submonolayer coverages on metal surfaces, the WF minimum is shifted with small amounts of O_2 down to 1.0–1.2 eV,[9,10,23,24] and comparable low WFs can be generated by the growth of thick layers involving Cs-O compounds.[25–28] Cs monoxide is often proposed to provide such low WFs,[25,29] but no clear relationship between the Cs/O ratios and the obtained WF has been found so far, i.e., it is unclear whether the formation of ultra-low WFs can be traced back to one specific oxide or rather a mixture and interplay of different oxides.[26,30–34] In addition to Cs oxides and hydroxides, the formation of Cs hydride (CsH) with the dissociated H atoms from the H_2O molecule is possible and might lead to a WF decrease of the order of 0.1 eV.[11,35]

The continuous accumulation of residual gases on caesiated surfaces under non-UHV conditions and in the absence of Cs evaporation leads to depolarization and passivation effects, causing an increase in the WF over time (typically called "Cs layer degradation").[17,36] The rate of increase depends on the base pressure, surface temperature, and initial WF. The degradation can be reversed by fresh Cs evaporation in a dedicated Cs conditioning procedure,[17] which needs to be performed at negative hydrogen ion sources after operational breaks.[37] In parallel to the evaporation of Cs, the converter surface at ion sources is simultaneously exposed to residual gas fluxes (mainly H_2O). Dedicated investigations on the WF evolution upon Cs and H_2O coadsorption do, however, barely exist. Indications of a beneficial impact of H_2O coadsorbates on the WF reduction were reported by Uebbing and James[25] in the context of photocathodes, where the exposure of an Ag substrate alternately to Cs and H_2O under UHV conditions led to a WF of 1.22 eV. Recently, it was shown that under high vacuum (HV) conditions of 10^{-6}–10^{-5} mbar (with H_2O being the main residual gas), the generation of ultra-low WFs in the range of 1.25 ± 0.10 eV is possible.[36,38] Moreover, at the caesiated ion source at J-PARC, it was demonstrated that the addition of H_2O helps to improve the source performance.[39]

In order to clarify the relevance of the base pressure in ion sources on the WF of the caesiated converter surface, investigations on Cs and water co-adsorption with different partial pressures of water are performed within this work. The investigations are conducted in a UHV chamber with a base pressure of $\sim 10^{-10}$ mbar, where different partial pressures of water are finely adjusted by using a leak valve. The WF is measured in absolute numbers by using the photoelectric effect. The obtained results are complemented by investigations performed at a separate experiment operating under a significantly higher base pressure of $\sim 10^{-6}$ mbar. The investigations at both experiments are done without the application of plasma. A polycrystalline molybdenum (Mo) surface is used as a substrate, as this is a typical material for converter surfaces at ion sources.[40–42] Since the converter surfaces at ion sources are usually operated at elevated temperatures, the influence of heating of the caesiated Mo substrates is investigated as well.

II. EXPERIMENTAL SETUPS

A. Ultra-high vacuum chamber

The UHV chamber is located at the Department of Physics at the University of Ioannina in Greece and is described in detail in Refs. 43 and 44. The chamber has a cylindrical shape with a height of 75 cm and diameter of 30 cm, which is pumped by an ion pump. The base pressure is of the order of 10^{-10} mbar and is continuously monitored with a pressure ion gauge. A quadrupole mass spectrometer (QMS) is used for residual gas analysis. Samples can be mounted on a rotatable, XYZ movable manipulator close to the center of the chamber and are fixed within a tantalum (Ta) foil case. Within this work, a polycrystalline Mo sample ($10 \times 10 \times 1$ mm^3) is used. The sample can be heated inductively by passing a current through a Ta ribbon uniformly pressed between the Ta case and the rear side of the sample. The temperature of the sample can be increased up to 1000 °C and is measured with a K-type thermocouple spot welded onto the case.

Cs deposition is carried out by evaporation from a commercial SAES Getters dispenser. The heating current of the dispenser is

varied between 5 and 6 A and the base pressure of the chamber does not change during the Cs deposition process, for which the sample is rotated in front of the dispenser. Prior to each Cs deposition, the dispenser is outgassed by keeping the operating current constant for about 1 min. The quantification of the Cs flux onto the surface is not possible, as this would require diagnostics such as tunable diode laser absorption spectroscopy (TDLAS)[45] or a quartz crystal microbalance,[46] which are currently not available at this setup. Controlled admission of water into the chamber is realized by using a variable leak valve connected to a canister of de-ionized water. Water vapor pressures of minimal 10^{-9} mbar up to 10^{-7} mbar were stably admitted within this work, and the water flux is kept constant during the caesiation of the sample.

The WF of the sample surface is measured in absolute numbers by applying a photoelectric WF diagnostic, which was developed at the Max Planck Institute for Plasma Physics (IPP) in Garching (Germany) and is described in detail in Ref. 37. Eight light-emitting diodes (LEDs) are used for the irradiation of the surface, providing mean photon energies in the range of 3.2–1.1 eV with a full width at half maximum (FWHM) of the LED spectra of 0.05–0.10 eV (measured with a spectrometer). As illustrated in Fig. 1, the LEDs (one at a time) are connected via an optical fiber to an achromatic lens head, which is placed in front of an optical viewport of the chamber. By rotating the sample in front of the viewport, the light is focused perpendicularly onto the sample surface with a spot diameter of about 6 mm. The photoelectrically emitted electrons are drawn onto an electrode made of Ta by applying a bias voltage of 75 V between the sample and the electrode. The electrode is placed in close proximity to the surface, and the currents for the different LEDs are measured one after the other with a picoammeter (Keithley 6487). The photocurrents are evaluated by subtraction of the dark current (measured when the surface is not irradiated), and the corresponding photoelectric yields are determined from the photocurrents by division by the LED-dependent relative intensity of the irradiated light onto the surface. The relative intensities are determined by measuring the radiant powers with a power meter (in the range of 3–8 mW) and converting them to photons/s. To evaluate the absolute WF, the photoelectric yield data are fitted according to the Fowler theory,[47] where the FWHM of the LED spectra are considered in the fitting routine. Typically, the three to four lowest photon energies with which the photoelectric signal is obtained are used for the evaluation of the WF, resulting in an uncertainty of ± 0.1 eV.[38] In case photoelectric signal is obtained with less than three LEDs, the WF is estimated as the mean value between the photon energy with which signal is obtained and the next lowest photon energy with which no signal is obtained, with a correspondingly higher error. Since photon energies above 3.2 eV were not available for the experiments, WFs $\gtrsim$3 eV cannot be evaluated. As mentioned above, the sample needs to be rotated in front of the viewport for the LED irradiation, which means that no Cs deposition takes place during the WF measurement. The WF measurement takes 1–2 min and the sample is rotated back after the measurement to continue the caesiation process.

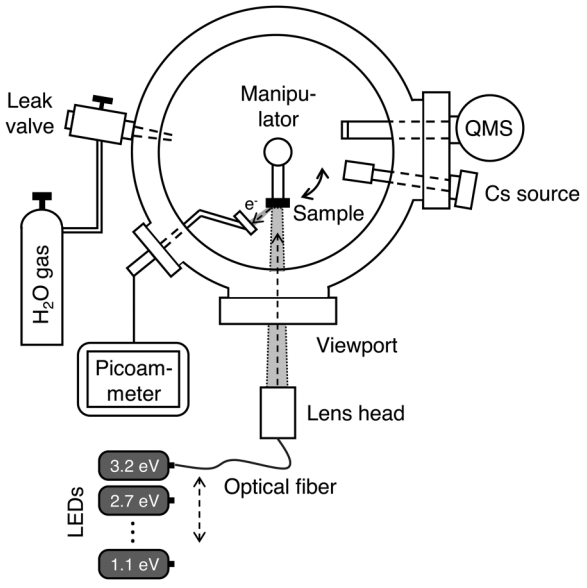

FIG. 1. Schematic of the UHV chamber including the photoelectric WF diagnostic.

B. High vacuum chamber

The high vacuum chamber (named ACCesS) is located at the University of Augsburg in Germany and is described in detail in Refs. 36 and 38. The ACCesS experiment is mainly dedicated to study the WF and H^- yield of caesiated surfaces exposed to low pressure low temperature hydrogen plasmas,[17,48] which are generated via inductive radio frequency (RF) coupling (27.12 MHz, 600 W max.). The cylindrical chamber is 15 cm in diameter and 10 cm in height and is evacuated with a turbomolecular pump to a base pressure of 10^{-6}–10^{-5} mbar (limited by Viton O-ring seals). The composition of the residual gas is measured with a differentially pumped residual gas analyzer (RGA), showing that it is clearly dominated by water vapor, i.e., the base pressure can be approximated by the partial pressure of H_2O. A sample holder is mounted close to the center of the chamber, where polycrystalline Mo substrates (3 µm Mo coating on a $30 \times 30 \times 5$ mm^3 Cu sample) are installed within this work. The samples can be heated up to 1000 °C and the temperature of the sample surface is measured with a K-type thermocouple clamped to the front surface.

To deposit Cs on the sample surface, a Cs oven is used that was designed and manufactured at IPP.[49] The Cs oven contains a liquid Cs reservoir (1 g Cs ampoule), which is heated to finely adjust the Cs evaporation rate. The density and temperature of the neutral Cs atoms in front of the surface are measured line-of-sight averaged by means of TDLAS.[45] From the TDLAS measurements, the isotropic neutral Cs flux can be calculated via $\Gamma_{Cs} = n_{Cs}\bar{v}_{Cs}/4$, where n_{Cs} is the neutral Cs density and $\bar{v}_{Cs}$ is the mean thermal velocity of the Cs atoms.

The absolute WF of the sample surface is measured by the same method as used in the UHV chamber (Fowler method). The applied WF setup is described in detail in Ref. 38. As tunable

light source, a high-pressure mercury lamp in combination with 20 interference filters (10 nm FWHM) is used, providing mean photon energies in the range of 5.0–1.5 eV. The radiation is focused with optical lenses through a quartz viewport perpendicularly onto the sample surface, resulting in a spot diameter of 15 mm (radiant powers ~0.1–1 mW). The photoemitted electrons are drawn to the grounded chamber walls by applying a bias of −30 V to the sample holder and surface, and the photocurrents are measured with the Keithley 6487 picoammeter. The available photon energies have recently been extended to 1.2 eV by using a high-pressure xenon lamp with corresponding interference filters, which enhances the WF threshold sensitivity down to ~1 eV. The LED-based WF measurement used at the UHV chamber was successfully benchmarked against the setup applied at ACCesS by giving an agreement of the determined WFs within ±0.1 eV.

III. RESULTS AND DISCUSSION

To ensure reproducibility, the polycrystalline Mo substrate is heated up to 1000 °C prior to each caesiation to remove adsorbed impurities and possibly Cs (compounds) from previous caesiations from the surface. After annealing, the WF is higher than 3.2 eV and expected to be equal to that of pure Mo, which is 4.3–4.6 eV.[5,6,8] The Cs deposition is started each time after the surface has cooled down to room temperature (RT).

A. Caesiation under UHV

To benchmark the photoelectric WF diagnostic, the Mo substrate is caesiated in the UHV chamber without the addition of H_2O to reproduce the characteristic WF minimum curve described in Sec. I. Figure 2(a) shows the WF plotted as a function of the Cs deposition time, with the base pressure being 4×10^{-10} mbar during the whole caesiation process. The surface is caesiated in time intervals of 30 s (dispenser current set to 6 A) and the WF is measured each time afterward. As can be seen, the WF decreases drastically by the deposition of Cs and reaches a minimum value of 1.45 ± 0.10 eV after 210 s. In Fig. 2(b), the corresponding photoelectric yields for the applied photon energies are plotted. The photoelectric yields are higher for higher photon energies and continuously increase until the WF minimum is reached. For Cs deposition times beyond 210 s, the photoelectric yields decrease and the evaluated WF increases, reaching 1.82 eV after 420 s. Hence, the measured behavior and absolute WF values are in excellent agreement with literature values,[8,9] and the growth of ~1 ML is expected. By repeating the measurements several times, it was confirmed that the minimum achievable WF is in the range of 1.5 ± 0.1 eV as indicated by the dashed bar in Fig. 2(a) (expected submonolayer regime) and that the maximum photoelectric yield is recorded at the WF minimum independently of the photon energy.

B. Caesiation at elevated water pressures

To investigate the WF evolution upon Cs and H_2O coadsorption, the caesiation procedure described in Sec. III A is performed with introducing H_2O into the UHV chamber. Different H_2O partial pressures are adjusted a few minutes before the caesiation of the Mo surface and are kept constant during the caesiation.

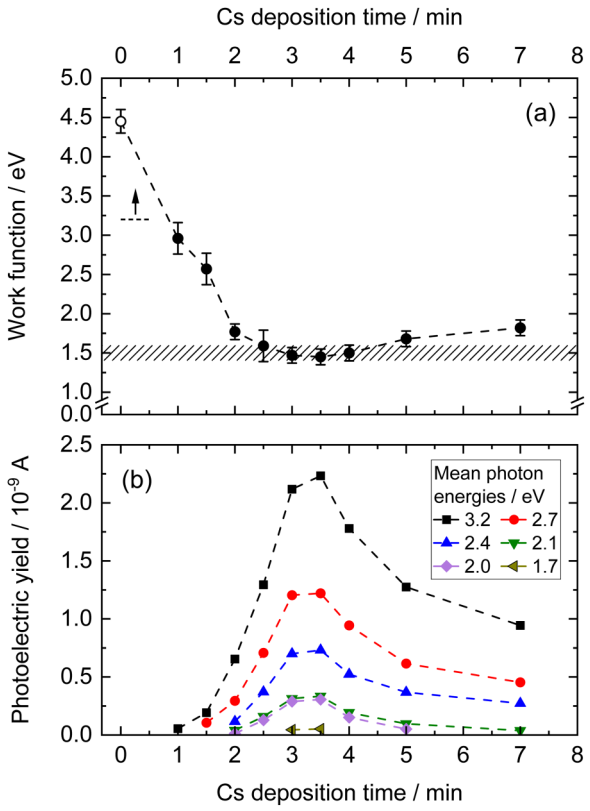

FIG. 2. Cs deposition on polycrystalline Mo under UHV conditions of 4×10^{-10} mbar at RT. In (a) the WF and in (b) the corresponding photoelectric yields for the applied photon energies are plotted as a function of the Cs deposition time. For Cs deposition times <60 s, the WF is >3.2 eV and cannot be evaluated with the current diagnostic setup (see text). The dashed bar in (a) indicates the range of measured WF minimum values in several analogous caesiation processes.

When the H_2O partial pressure is $\sim 10^{-9}$ mbar in the chamber, the WF evolution is the same as shown in Fig. 2. By increasing the pressure to $\sim 10^{-8}$ mbar, however, the WF behaves differently. This is shown in Fig. 3, where the WF evolution at $\sim 10^{-8}$ mbar is compared to the data from Fig. 2(a) (circular symbols). As can be seen, the reduction in WF is slowed down, and after 210 s, where without the addition of H_2O the WF minimum of 1.5 eV is reached, the WF is between 2.2 and 1.8 eV. By increasing the caesiation time, the WF does not increase but reaches a value of 1.55 eV after 6 min and decreases further to ultra-low values of below 1.5 eV for caesiation times longer than 8 min. After 16 min, a WF of 1.13 eV is reached. This WF is stable for prolonged Cs deposition times up to 21 min. By repeating the measurements it was confirmed that stable WFs in the range of 1.2 ± 0.1 eV are reached at 10^{-8} mbar partial water pressure, indicated by the blue dashed bar in Fig. 3.

The inset graph in Fig. 3 shows typical photoelectric yield curves corresponding to the WF minimum of 1.5 eV achieved without introduction of H_2O and to the ultra-low WF close to

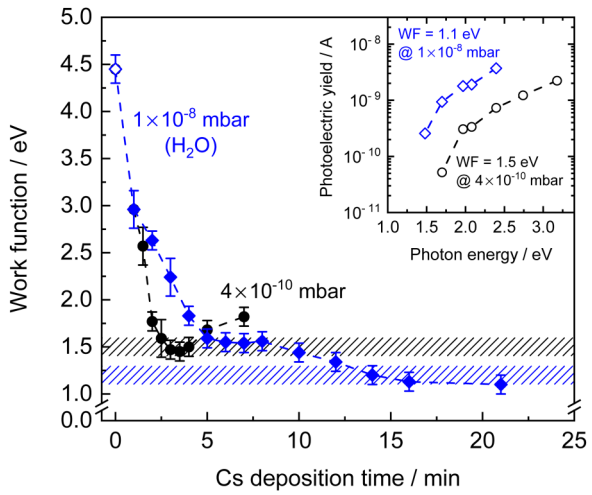

FIG. 3. WF of the polycrystalline Mo surface upon caesiation at RT under 1×10^{-8} mbar water partial pressure ultra-low. The data shown in Fig. 2(a) are additionally plotted for comparison (circular symbols). The dashed bars indicate the range of measured WF minimum values in several analogous caesiation processes. The inset graph shows typical photoelectric yield curves for the minimum WFs achieved with the two different base pressures.

1.1 eV with 10^{-8} mbar H_2O. Apart from the extension of the photoelectric response to the near infrared (1.5 eV) at 10^{-8} mbar, the photoyield is increased by more than one order of magnitude at 1.7 eV and by almost one order of magnitude for the higher photon energies. Hence, the reduction in WF is accompanied by a general increase in the photoelectric quantum efficiency (QE) of the surface.

The lower WF and higher QE achieved in the water environment clearly show that the chemical composition of the surface is changed. While at 10^{-9} mbar, the H_2O flux onto the surface seems to be negligible with regard to the WF evolution, the WF reduction and therefore the generation of strong electric dipoles on the surface in the initial caesiation phase are slightly hampered at 10^{-8} mbar. However, after a critical Cs fluence and thus Cs coverage on the substrate is obtained, the formation of ultra-low WFs is enabled. The coadsorption of Cs and H_2O at the surface presumably enhances the partial and/or full water dissociation at the surface, which opens the pathways for the formation of Cs oxides, as explained in Sec. I. A Langmuir–Hinshelwood mechanism is proposed for these reactions, in which the negative enthalpy of formation of Cs oxides thermodynamically favors the oxidation of Cs.[44] Unfortunately, the chemical composition of the surface cannot be analyzed because *in situ*/*operando* surface analysis techniques [such as x-ray photoelectron spectroscopy (XPS), Auger electron spectroscopy (AES), or Fourier transform infrared spectroscopy (FTIR)] are not available at present, and an *ex situ* analysis is not meaningful due to pronounced changes of the surface composition as soon as the substrate is exposed to air [high reactivity of the strongly deliquescent/hygroscopic Cs (compounds)]. Since Cs compounds have a substantially lower vapor pressure compared to pure Cs,[50,51] the Cs-water coadsorption allows the formation of multilayers on the substrate at room temperature,[44,46] which is probably the case in the extended Cs deposition time up to 21 min in Fig. 3.

By increasing the H_2O partial pressure to $\sim 10^{-7}$ mbar, the WF is only reduced to ~2 eV with the usually applied Cs dispenser current. However, by increasing the dispenser current and thus the Cs evaporation rate, ultra-low WFs down to 1.27 eV are achieved again. Therefore, the flux ratio of Cs to H_2O onto the surface is a critical parameter for the generation of ultra-low WF layers. This is confirmed by investigations performed at the ACCesS experiment, where the base pressure is in the range of HV (10^{-6}–10^{-5} mbar) and the Cs flux onto the surface can be finely adjusted and quantified by means of the TDLAS system. Figure 4 shows a compilation of WF data from several caesiations at ACCesS, where the different caesiations (indicated by different symbols) demonstrate an excellent reproducibility.[36] The WF is plotted as a function of the Cs to H_2O flux ratio onto the surface, where the H_2O flux is the thermal flux calculated from the base pressure. Similar to the experiments in the UHV chamber, ultra-low WFs in the range of 1.25 ± 0.10 eV are reliably generated. The ultra-low WF is achieved when the Cs to H_2O flux ratio onto the surface exceeds the threshold $\Gamma_{Cs/H_2O} \gtrsim 5 \times 10^{-3}$, i.e., the stoichiometry of Cs and H_2O on the surface is decisive.

When the Cs to H_2O flux ratio is reduced and/or the Cs deposition is stopped, the Cs layer degrades and the WF typically increases over time. At the vacuum level of $\sim 10^{-10}$ mbar in the UHV chamber, however, no degradation is observed up to 14 h as can be seen in Fig. 5. In contrast, under HV conditions, the WF

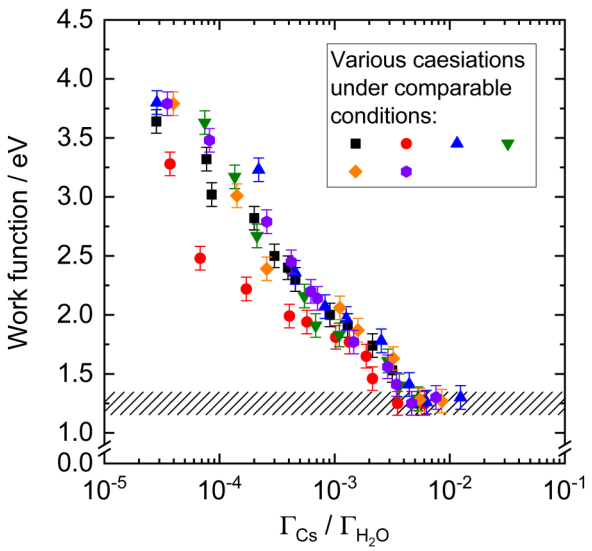

FIG. 4. Compilation of WF data for various caesiations of polycrystalline Mo surfaces at RT at the high vacuum chamber ACCesS, with the different symbols representing different caesiations. The WF is plotted as a function of the flux ratio of Cs atoms to residual water molecules onto the surface. Adapted with permission from Heiler *et al.*, JINST **19**, C01057 (2024). Copyright (2024) IOP Publishing under a Creative Commons License.

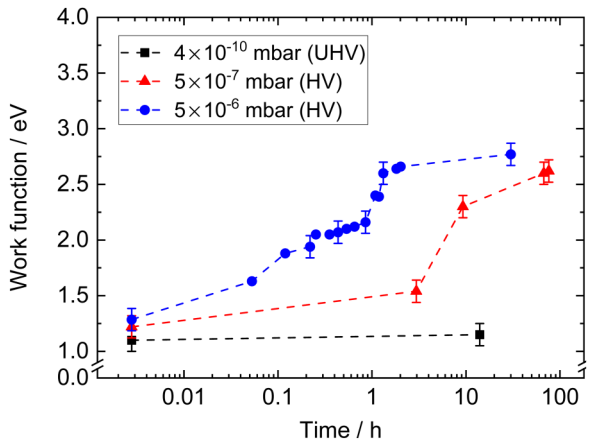

FIG. 5. WF degradation of ultra-low WF layers exposed to different base pressures (UHV and HV conditions) at RT.

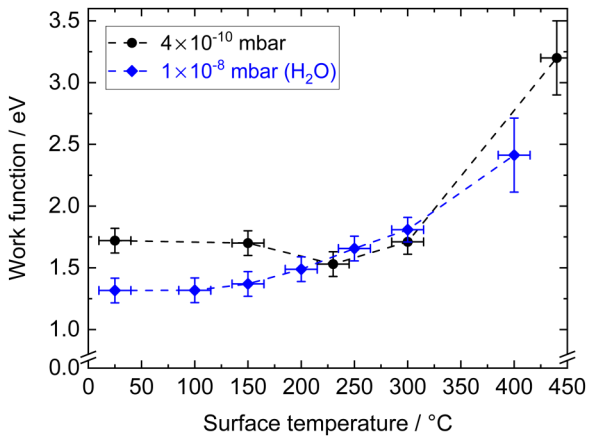

FIG. 6. WF of caesiated polycrystalline Mo surfaces in dependence of elevated surface temperatures without Cs flux toward the surface. The caesiation is done before increasing the surface temperature under UHV conditions of 4×10^{-10} mbar (pure Cs layer) as well as with a water partial pressure of 1×10^{-8} mbar for the generation of an ultra-low WF layer.

after 14 h is about 2.4 and 2.7 eV at base pressures of 5×10^{-7} and 5×10^{-6} mbar, respectively.

C. Impact of elevated surface temperatures

The converter surface in negative hydrogen ion sources for accelerators and fusion is usually temperature controlled. The optimum temperature is determined empirically and is in the range of 125–150 °C at RF driven ion sources for fusion.[42,52] In this work, the influence of the temperature on the WF of caesiated surfaces is systematically investigated. Before the temperature of the sample is increased, the sample is caesiated until a stable WF is reached. Afterward, the caesiation is stopped and the sample is heated stepwise. To measure the WF, the heating is paused to not disturb the WF measurement by electromagnetic interference. The results are shown in Fig. 6, where the WF is plotted as a function of the surface temperature. The measurements are performed under UHV conditions without water admission (4×10^{-10} mbar) as well as with water admission (1×10^{-8} mbar) to generate the ultra-low WF layer.

The measurements without water admission start with a WF value of 1.7 eV, which is achieved by caesiation past the WF minimum (see Fig. 2). By heating the surface up to 200 °C, the WF remains constant within the error bars. At 230 °C, the WF decreases to a value of 1.5 eV. For higher temperatures, the WF increases. This behavior is explained by the removal of Cs from the surface for temperatures above 200 °C. Due to the assumed desorption of Cs the surface coverage is reduced, and the caesiation curve from Fig. 2(a) is reversed including the typical WF minimum value for Cs submonolayers.

In case of the measurements with water admission, the sample is caesiated until a WF of 1.3 eV is reached. Again, for temperatures up to 200 °, the measured WF remains constant within the error bars. Above 200 °C, however, the WF increases. The WF increase indicates thermally induced changes of the chemical composition of the surface, and desorption of Cs from the surface is expected.

In order to confirm the hypothesis of Cs desorption above 200 °C, measurements are performed at the ACCesS experiment, where the neutral Cs density above the surface can be measured by means of TDLAS. In Fig. 7, measurements are shown after the Mo sample was caesiated to a WF of 1.2 eV and degraded to 3.3 eV afterward by stopping the Cs evaporation and leaving the surface in vacuum for several days. The sample is heated stepwise up to 890 °C while the neutral Cs density in front of the sample is measured via TDLAS. For temperatures below 200 °C, no Cs is detected.

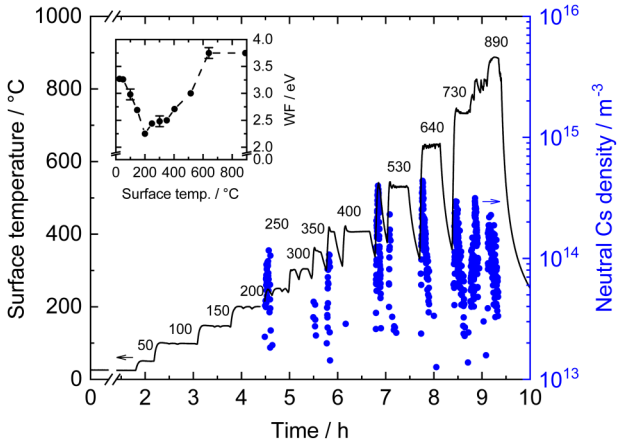

FIG. 7. Heat treatment of a degraded caesiated polycrystalline Mo surface without Cs flux toward the surface at ACCesS (base pressure 5×10^{-6} mbar): The surface temperature and the measured neutral Cs density desorbed from the surface are plotted over time. The inset graph shows the dependence of the WF on the surface temperature.

When the surface temperature is increased beyond 200 °C, however, Cs is measured in front of the surface during the ramp up phases of the surface temperature. The different temperature steps lead to recurrent Cs desorption, showing that the Cs atoms have different binding energies at the surface.

The WF is measured at each temperature step and is plotted in the inset graph in Fig. 7. As can be seen, temperatures above 50 °C lead to a WF reduction of the degraded Cs layer. At 200 °C, the WF is 2.25 ± 0.10 eV and thus more than 1 eV lower than before the heating. Up to this point, thermal desorption of Cs is not detected, but RGA measurements reveal that residual gases (mainly H_2O) are thermally desorbed from the surface. By increasing the temperature to 250 °C and above, the measured Cs desorption is accompanied by an increase in the WF. Hence, the results demonstrate that the Cs desorption from the surface for temperatures above 200 °C affects the chemical composition of the surface and leads to an increase in the WF under the given conditions.

IV. CONCLUSIONS AND OUTLOOK

An experimental study of Cs and water coadsorption on polycrystalline Mo at different partial pressures of water using two different experimental setups has been carried out. Under UHV conditions of $\sim 10^{-10}$ mbar, the widespread characteristic WF curve is confirmed, with the minimum WF being in the range of 1.5 ± 0.1 eV corresponding to a submonolayer coverage of Cs. When the water vapor partial pressure is increased to $\sim 10^{-9}$ mbar, the WF behavior does not change, and the same typical submonolayer WF minimum is still measured. By increasing the water partial pressure to 10^{-8} mbar and beyond, however, a different WF behavior is given and even lower WF values down to 1.1 eV are reached, accompanied by a significantly enhanced QE of the surface. The ultra-low WF is attributed to the formation of Cs oxides at the surface, and the increased QE indicates a higher electron density at the Fermi edge of the surface. The lower WF and higher QE are expected to be highly beneficial with regard to the surface production of negative hydrogen ions.[53] The formation of the ultra-low WF layer is dependent on the flux ratio of Cs atoms to water molecules onto the surface, i.e., at rather low base pressures of 10^{-8} mbar less Cs needs to be consumed to achieve the ultra-low WF.

Apart from the fact that the minimum WF under UHV conditions is higher compared to that achieved with water admission, a Cs submonolayer has the disadvantage that maintaining the optimum Cs coverage is challenging, especially at negative hydrogen ion sources for fusion with their large converter surfaces of up to 2 m^2. One also needs to consider that in ion sources, the surface is exposed to the plasma interaction. This makes maintaining a stable WF in the submonolayer regime even more challenging. With the presence of water, the Cs coating can get several ML in thickness depending on the applied Cs fluence, as Cs compounds have a substantially lower vapor pressure than pure Cs. The preparation of thick coatings in the vacuum phase makes the resulting WF widely independent from the substrate material and is a valuable countermeasure for the plasma-induced removal of Cs (compounds) from the surface.

Temperatures above 200 °C are detrimental for ultra-low WF layers achieved by Cs and water coadsorption. The WF starts to increase and the performed investigations at different base pressures have shown that Cs is significantly desorbed. In consequence, the temperature of the converter surface in ion sources should not exceed 200 °C independent of the base pressure.

On balance, the presented investigations confirm the beneficial impact of Cs and water coadsorption on the WF reduction of surfaces. The base pressure foreseen for the negative hydrogen ion sources for the ITER neutral beam injectors is 10^{-8} mbar and hence still sufficient to decrease the WF to ultra-low values in the vacuum phase. Future investigations will focus on the deposited layer thickness by using a quartz crystal microbalance. Since the WF is crucially dependent on the chemical composition of the converter surface, XPS and FTIR measurements will also be considered for the chemical analysis of the surface. In addition, the impact of hydrogen plasma interaction on surfaces prepared with Cs and water coadsorption will be further investigated.

ACKNOWLEDGMENTS

This work has been carried out within the framework of the EUROfusion Consortium, funded by the European Union via the Euratom Research and Training Programme (Grant Agreement No. 101052200 - EUROfusion). Views and opinions expressed are, however, those of the authors only and do not necessarily reflect those of the European Union or the European Commission. Neither the European Union nor the European Commission can be held responsible for them.

AUTHOR DECLARATIONS

Conflict of Interest

The authors have no conflicts to disclose.

Author Contributions

A. Heiler: Conceptualization (lead); Data curation (equal); Formal analysis (equal); Investigation (equal); Methodology (equal); Project administration (equal); Validation (equal); Visualization (lead); Writing – original draft (lead). **N. Klose:** Conceptualization (supporting); Data curation (equal); Formal analysis (equal); Investigation (equal); Methodology (equal); Validation (equal); Visualization (supporting); Writing – original draft (supporting). **R. Friedl:** Conceptualization (supporting); Writing – review & editing (equal). **U. Fantz:** Conceptualization (supporting); Funding acquisition (equal); Project administration (equal); Writing – review & editing (equal). **D. Vlachos:** Conceptualization (supporting); Funding acquisition (equal); Project administration (equal); Supervision (lead); Writing – review & editing (equal).

DATA AVAILABILITY

The data that support the findings of this study are available from the corresponding author upon reasonable request.

REFERENCES

[1]T. Aruga and Y. Murata, Prog. Surf. Sci. **31**, 61 (1989).
[2]R. D. Diehl and R. McGrath, Surf. Sci. Rep. **23**, 43 (1996).

[3]A. G. Naumovets, "Adsorption of Alkali and other electropositive metals," in *Surface and Interface Science* (John Wiley & Sons, Ltd, Weinheim, 2016), Chap. 34, p. 157.
[4]M. Bacal and M. Wada, Appl. Phys. Rev. **2**, 021305 (2015).
[5]*CRC Handbook of Chemistry and Physics*, 103rd ed., edited by J. R. Rumble (CRC/Taylor & Francis, Boca Raton, FL, 2022).
[6]H. B. Michaelson, J. Appl. Phys. **48**, 4729 (1977).
[7]R. G. Wilson, J. Appl. Phys. **37**, 3161 (1966).
[8]R. G. Wilson, J. Appl. Phys. **37**, 4125 (1966).
[9]L. W. Swanson and R. W. Strayer, J. Chem. Phys. **48**, 2421 (1968).
[10]C. A. Papageorgopoulos, Phys. Rev. B **25**, 3740 (1982).
[11]M.-L. Ernst-Vidalis, M. Kamaratos, and C. Papageorgopoulos, Surf. Sci. **189–190**, 276 (1987).
[12]R. D. Diehl and R. McGrath, J. Phys.: Condens. Matter **9**, 951 (1997).
[13]M. Scheffler and C. Stampfl, "Theory of adsorption on metal substrates," in *Handbook of Surface Science*, edited by K. Horn and M. Scheffler (Elsevier, Amsterdam, 2000), Vol. 2, pp. 285.
[14]T. A. Flaim and P. D. Ownby, Surf. Sci. **32**, 519 (1972).
[15]S. H. Chou, J. Voss, I. Bargatin, A. Vojvodic, R. T. Howe, and F. Abild-Pedersen, J. Phys.: Condens. Matter **24**, 445007 (2012).
[16]U. Fantz *et al.*, Nucl. Fusion **64**, 086063 (2024).
[17]A. Heiler, R. Friedl, and U. Fantz, Plasma Chem. Plasma Process. **45**, 1 (2025).
[18]M. Sudolská, L. Cantrel, and I. Černušák, J. Mol. Model. **20**, 2218 (2014).
[19]G. Pirug, C. Ritke, and H. P. Bonzel, Surf. Sci. **257**, 50 (1991).
[20]H. Shi and K. Jacobi, Surf. Sci. **317**, 45 (1994).
[21]M. A. Henderson, Surf. Sci. Rep. **46**, 1 (2002).
[22]H. Okamoto, J. Phase Equilibria Diffus. **31**, 86 (2010).
[23]C. A. Papageorgopoulos and J. M. Chen, Surf. Sci. **39**, 313 (1973).
[24]J.-L. Desplat and C. A. Papageorgopoulos, Surf. Sci. **92**, 97 (1980).
[25]J. J. Uebbing and L. W. James, J. Appl. Phys. **41**, 4505 (1970).
[26]T. R. Briere and A. H. Sommer, J. Appl. Phys. **48**, 3547 (1977).
[27]L. R. Danielson, J. Appl. Phys. **52**, 300 (1981).
[28]S. T. Melnychuk and M. Seidl, J. Vac. Sci. Technol. A **9**, 1650 (1991).
[29]J.-L. Desplat, J. Appl. Phys. **54**, 5494 (1983).
[30]P. E. Gregory, P. Chye, H. Sunami, and W. E. Spicer, J. Appl. Phys. **46**, 3525 (1975).
[31]G. Ebbinghaus and A. Simon, Chem. Phys. **43**, 117 (1979).
[32]S.-J. Yang and C. W. Bates, Jr., Appl. Phys. Lett. **36**, 675 (1980).
[33]B. Woratschek, W. Sesselmann, J. Küppers, G. Ertl, and H. Haberland, J. Chem. Phys. **86**, 2411 (1987).
[34]A. Band, A. Albu-Yaron, T. Livneh, H. Cohen, Y. Feldman, L. Shimon, R. Popovitz-Biro, V. Lyahovitskaya, and R. Tenne, J. Phys. Chem. B **108**, 12360 (2004).
[35]B. S. Rump and B. L. Gehman, J. Appl. Phys. **36**, 2347 (1965).
[36]A. Heiler, R. Friedl, and U. Fantz, J. Instrum. **19**, C01057 (2024).
[37]A. Heiler, C. Wimmer, J. Berner, and U. Fantz, J. Phys.: Conf. Ser. **2743**, 012025 (2024).
[38]A. Heiler, R. Friedl, and U. Fantz, AIP Adv. **12**, 035339 (2022).
[39]A. Ueno, J. Phys.: Conf. Ser. **2743**, 012001 (2024).
[40]M. Bacal, Nucl. Fusion **46**, S250 (2006).
[41]D. Faircloth and S. Lawrie, New J. Phys. **20**, 025007 (2018).
[42]U. Fantz, S. Briefi, A. Heiler, C. Wimmer, and D. Wünderlich, Front. Phys. **9**, 709651 (2021).
[43]D. Vlachos, E. Giotopoulou, S. D. Foulias, and M. Kamaratos, Mater. Res. Express **2**, 116501 (2015).
[44]M. Kamaratos, E. Giotopoulou, and D. Vlachos, React. Kinet., Mech. Catal. **135**, 3257 (2022).
[45]U. Fantz and C. Wimmer, J. Phys. D: Appl. Phys. **44**, 335202 (2011).
[46]U. Fantz, R. Gutser, and C. Wimmer, Rev. Sci. Instrum. **81**, 02B102 (2010).
[47]R. H. Fowler, Phys. Rev. **38**, 45 (1931).
[48]S. Cristofaro, R. Friedl, and U. Fantz, Plasma **4**, 94 (2021).
[49]S. Cristofaro, M. Fröschle, A. Mimo, A. Rizzolo, M. De Muri, M. Barbisan, and U. Fantz, Rev. Sci. Instrum. **90**, 113504 (2019).
[50]J. B. Taylor and I. Langmuir, Phys. Rev. **51**, 753 (1937).
[51]S. P. Berardinelli and D. L. Kraus, Inorg. Chem. **13**, 189 (1974).
[52]C. Wimmer, A. Mimo, M. Lindauer, U. Fantz, and the NNBI-Team, AIP Conf. Proc. **2011**, 060001 (2018).
[53]B. Rasser, J. N. M. van Wunnik, and J. Los, Surf. Sci. **118**, 697 (1982).